# Electrochemical Random Signal Analysis during Localized Corrosion of Anodized 1100 Aluminum Alloy in Chloride Environments

**M. Sakairi[1,†], Y. Shimoyama[1], and D. Nagasawa[2]**

[1]*Graduate School of Engineering, Hokkaido University*
*Kita-13, Nishi-8, Kita-ku, Sapporo, 060-8628, Japan*
[2]*Nippon light metal co. ltd.*
*1-34-1 Kanbara, Kanbara-cho, Shizuoka-ken, 421-3291, Japan*

A new type of electrochemical random signal (electrochemical noise) analysis technique was applied to localized corrosion of anodic oxide film formed 1100 aluminum alloy in 0.5 kmol/m$^3$ H$_3$BO$_4$/0.05 kmol/m$^3$ Na$_2$B$_4$O$_7$ with 0.01 kmol/m$^3$ NaCl. The effect of anodic oxide film structure, barrier type, porous type, and composite type on galvanic corrosion resistance was also examined. Before localized corrosion started, incubation period for pitting corrosion, both current and potential slightly change as initial value with time. The incubation period of porous type anodic oxide specimens are longer than that of barrier type anodic oxide specimens. While pitting corrosion, the current and potential were changed with fluctuations and the potential and the current fluctuations show a good correlation. The records of the current and potential were processed by calculating the power spectrum density (PSD) by the Fast Fourier Transform (FFT) method. The potential and current PSD decrease with increasing frequency, and the slopes are steeper than or equal to minus one (-1). This technique allows observation of electrochemical impedance changes during localized corrosion.

***Keywords*** *: galvanic corrosion, aluminum, anodizing, electrochemical noise, chloride ions.*

## 1. Introduction

Because of their high strength-weight ratio and high corrosion resistance, aluminum and its alloys are widely used, for example, automotive, containers and house wear etc. In specific applications, they are sometimes joined to other metals such as iron and cupper. Galvanic corrosion may occur in such situations and this is a very severe problem to the durability of some systems.

Aluminum and its alloys are sometimes used without any surface treatment. However, aluminum and its alloys are also used after surface treatment processing, such as anodizing and painting. There are two types of anodic oxide films, a porous type and a barrier type that can be formed on aluminum.[1]-[5] The barrier type anodic oxide film has an amorphous structure[6] and the thickness depends on the anodizing potential or voltage. The porous type anodic oxide film has an outer porous layer and an inner barrier layer.[7] The porous layer thickness increases

linearly with anodizing time and the barrier layer thickness is dependent on anodizing solution and current density. Fig. 1 shows schematic representation of both type anodic oxide film thickness change with potential and anodizing time. Barrier type anodic oxide films are mainly used in dielectric substance of electrolytic capacitors, and porous type anodic oxide films as protective film for corrosion resistance and for creating micro structures[7]-[11] or molds.[12]-[14] Therefore anodic oxide film structure and dielectric property are well investigated. There are few papers focused on corrosion of aluminum, especially effect of anodic oxide film structure and thickness on corrosion protection of aluminum. The extent of the effect of the anodizing surface treatment on the galvanic corrosion of aluminum and its alloys joined to other dissimilar alloys has not been established.

Recently, an electrochemical random signal (noise) analysis technique has been applied in a number of corroding environments.[15]-[21] Bertocci et al.[15],[16] has reported a electrochemical noise technique employing a corrosion couple and FFT (Fast Fourier Transformation). Traditional

---
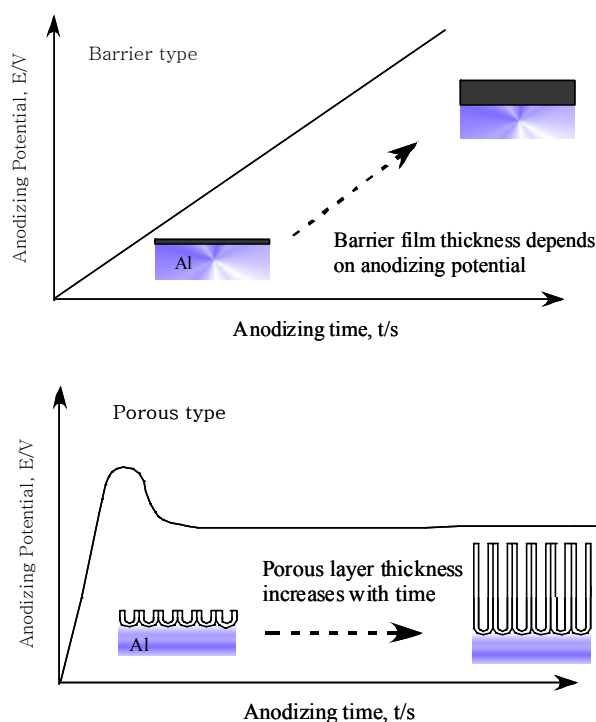† Corresponding author: msakairi@eng.hokudai.ac.jp

**Fig. 1.** Schematic representation of both type anodic oxide film thickness change with potential and anodizing time.

electrochemical impedance techniques are not suitable to measure the impedance during galvanic corrosion, but, this new noise technique can obtain the impedance even with localized corrosion, because the impedance is calculated using a power spectrum density (PSD) of the current and potential. Sakairi et al reported influence of anodic oxide film structure on electrochemical impedance which was calculated by using FFT during galvanic corrosion of highly pure aluminum and 6061 alloy.[22),23)]

The purpose of this study is to apply the new electrochemical noise technique to galvanic corrosion of anodized 1100 aluminum alloy and to examine the effect of anodic oxide film structure, barrier, porous and composite types, on the electrochemical impedance during galvanic corrosion.

# 2. Experimental

## 2.1 Specimen

1100 aluminum alloy sheets were cut to 20x30 mm$^2$ with a handle. The specimens were cleaned in ethanol and in doubly distilled water in an ultrasonic bath.

## 2.2 Anodizing

Barrier type anodic oxide films, Type I, were formed by anodizing at 293 K in 0.5 kmol/m$^3$ H$_3$BO$_4$ / 0.05 kmol/m$^3$ Na$_2$B$_4$O$_7$ solutions with constant current density,

$i_a = 10$ A/m$^2$, and then with a constant potential, $E_a = 50$ V for 1.8 ks. Porous type anodic oxide films, Type II, were formed by anodizing at 263 K in 3.72 kmol/m$^3$ H$_2$SO$_4$ solutions with a constant current density, $i_a = 100$ A/m$^2$ for 600 s. Composite type anodic oxide films, Type III, were formed by anodizing initially in 3.72 kmol/m$^3$ H$_2$SO$_4$ solutions at 263 K and re-anodized in 0.5 kmol/m$^3$ H$_3$BO$_4$ / 0.05 kmol/m$^3$ Na$_2$B$_4$O$_7$ solutions.

After anodizing, specimen edges were sealed again by silicon resin and the exposes area to the solution was 1 cm$^2$.

## 2.3 Electrochemical measurement

Specimens were dipped in 0.5 kmol/m$^3$ H$_3$BO$_4$ / 0.05 kmol/m$^3$ Na$_2$B$_4$O$_7$ solutions with 0.3 kmol/m$^3$ NaCl, and connected with a 16 cm$^2$ Pt plate (artificial cathode) as a counter electrode, to form a galvanic couple. The galvanic current between specimen and counter electrode, and the specimen potential during the test were measured by a computer through an A/D converter and signal was measured at one second intervals. The records of the current and potential were processed by calculating the power spectrum density (PSD) with the FFT method. To calculate PSD, a rectangular window was used. The electrochemical noise impedance was calculated from the current PSD and potential PSD values.

A saturated Ag/AgCl electrode was used as the reference electrode in the measurements of the specimens potential during galvanic corrosion tests.

## 2.4 Surface observations

The specimen surfaces were examined by confocal scanning laser microscopy (CSLM; Laser Tech. Co. 1SA-21) and scanning electron microscopy (SEM; JEOL, FE-6500F) after the anodizing and the galvanic corrosion tests.

# 3. Results and discussion

## 3.1 Anodizing behavior

Fig. 2 shows changes in current and potential during anodizing, Type I, in 0.5 kmol/m$^3$ H$_3$BO$_4$ / 0.05 kmol/m$^3$ Na$_2$B$_4$O$_7$ solutions. While constant current anodizing, potential increases with time and current decreases suddenly after changing constant potential mode. The slope of the potential curve of 1100 alloy was steeper than that of highly pure aluminum. This result suggests that the almost same barrier type oxide film of highly pure aluminum formed on 1100 alloy, and the thickness is also almost same as highly pure aluminum. The anodizing ratio nm/V in this anodizing condition is about 1.5 nm/V, therefore the oxide film thickness is about 75 nm. However, the
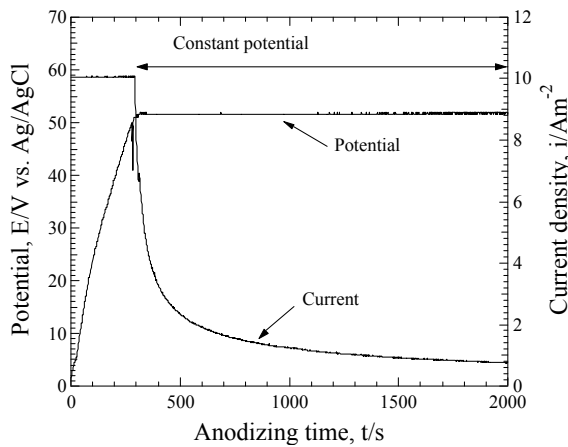
**Fig. 2.** Changes in current and potential during anodizing, Type I, in 0.5 kmol/m$^3$ H$_3$BO$_4$ / 0.05 kmol/m$^3$ Na$_2$B$_4$O$_7$ solutions.



**Fig. 4.** Changes in the current and the potential with immersion time during galvanic corrosion of Pt coupled to without anodized specimen in 0.5 kmol/m$^3$ H$_3$BO$_3$ / 0.05 kmol/m$^3$ Na$_2$B$_4$O$_7$ with 0.3 kmol/m$^3$ NaCl.

number of defects in the oxide film of 1100 alloy may be larger than that of highly pure aluminum. The anodizing behaviors for another oxide films, type II and III, were almost same as highly pure aluminum, these results also indicated that Type II and Type III films structure were also same as these formed on highly purer aluminum.

Fig. 3 shows CSLM contrast images of specimens surface after anodizing in each conditions. Because of oxide film thickness and aluminum anodic oxide films are almost transparent, the surface morphology of Type I film formed specimen is almost same as before anodizing. On the other hand, the morphology of Type II and Type III film formed specimens have a lot of dark spot. These are may be second phase particle inside the substrate. Some of the second phase particle may be remain inside the oxide film. Because of Type II and Type III oxide films are also transparent, these particles may be observed by CSLM.[24]
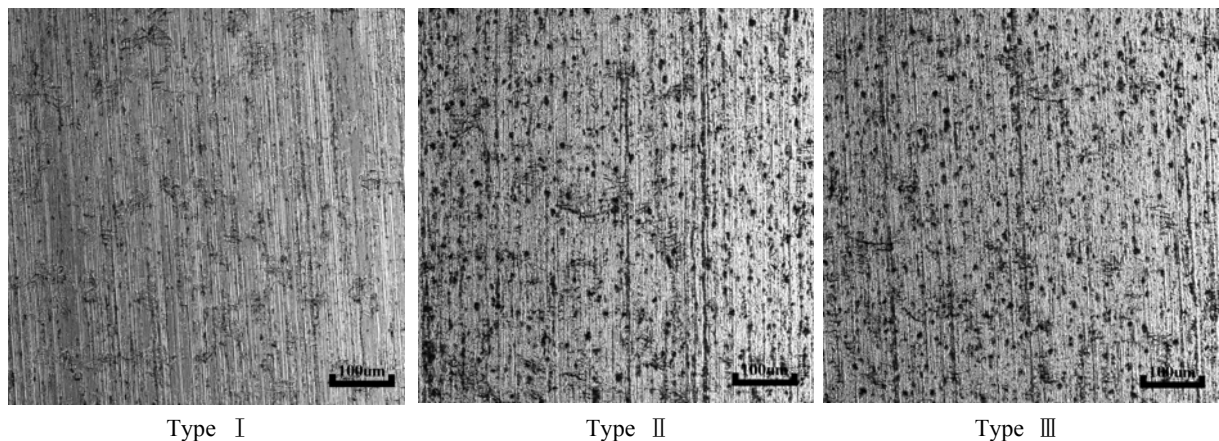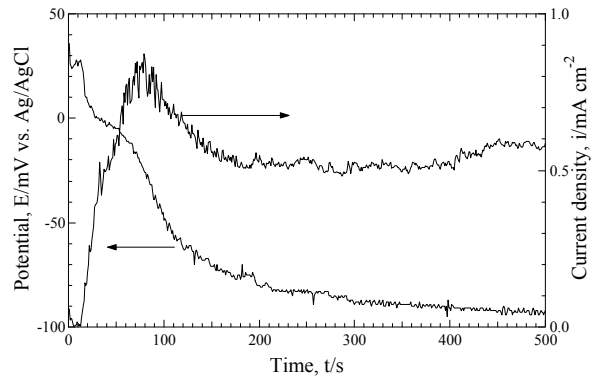
## 3.2 Galvanic corrosion

Fig. 4 shows changes in the current and the potential with immersion time during galvanic corrosion of Pt coupled to without anodized specimen in 0.5 kmol/m$^3$ H$_3$BO$_3$ / 0.05 kmol/m$^3$ Na$_2$B$_4$O$_7$ with 0.3 kmol/m$^3$ NaCl. As specimen connected to the Pt electrode, the potential changes to negative direction with fluctuation and the current increases with fluctuations. These fluctuation may be related to localized corrosion, pitting corrosion. After the test, specimen surface was covered by corrosion products, and after removed corrosion product, pits were existed.

Fig. 5 shows changes in the current and the potential with immersion time during galvanic corrosion of Pt coupled to Type III specimen in 0.5 kmol/m$^3$ H$_3$BO$_3$ / 0.05 kmol/m$^3$ Na$_2$B$_4$O$_7$ with 0.3 kmol/m$^3$ NaCl. During the incubation period (< 500 s), neither current nor potential changes from the initial values, however, after 500 s, there
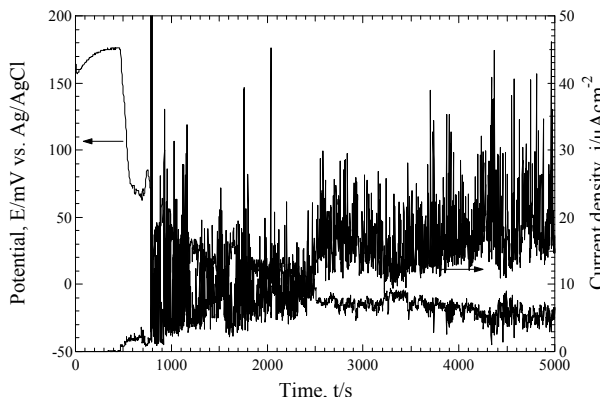


| Type I | Type II | Type III |

**Fig. 3.** CSLM contrast images of specimens surface after anodized.

**Fig. 5.** Changes in the current and the potential with immersion time during galvanic corrosion of Pt coupled to Type III specimen in 0.5 kmol/m$^3$ H$_3$BO$_3$ / 0.05 kmol/m$^3$ Na$_2$B$_4$O$_7$ with 0.3 kmol/m$^3$ NaCl.
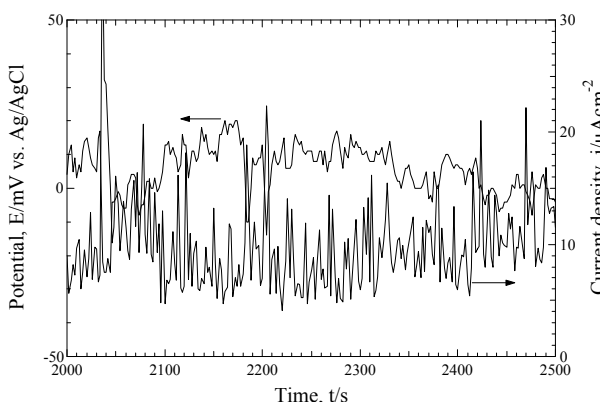


**Fig. 6.** Magnification of the potential and current in Fig. 5 after the localized corrosion has started.

are sudden changes as indicated by the electrochemical random signal fluctuations. The incubation period increased in the order of Type I specimen, Type II specimen, Type III specimen. The localized corrosion and pitting corrosion are stochastic phenomena, however, this behavior is very similar in all experiments.

Fig. 6 is a magnification of the potential and current in Fig. 5 after the localized corrosion has started, showing that the potential and current move in opposite directions with good correlation. The current and potential fluctuations may be related to individual events in the generation, growth, and extinction of localized or pitting corrosion. The computed pit size using the current fluctuations suggests pits of several tens μm, when the shape of a pit is hemispherical and aluminum dissolves as Al$^{3+}$.

**3.3 PSD of electrochemical random signal and impedance**

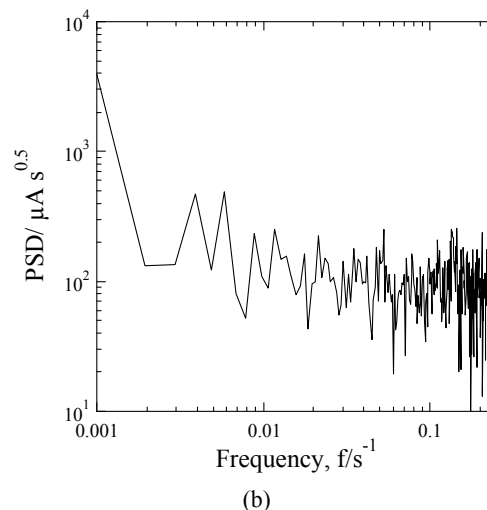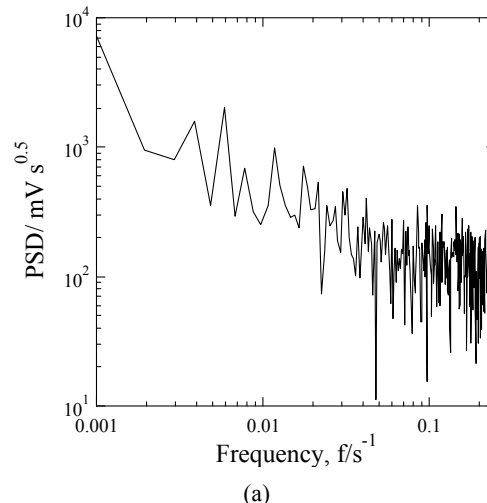Fig. 7 shows the PSD of the a) potential and b) current



(a)



(b)

**Fig. 7.** Power spectrum density (PSD) of the a) potential and b) current in Fig 6.

in Fig. 6. The potential PSD decrease with increasing frequency, and the slopes are steeper than or equal to -1. The current PSD slightly decreases with increasing frequency. A slope -1 indicates that each event, each pitting corrosion event, occurs independent of other events.

The electrochemical impedance can be computed by using the potential and current PSD.

$$Z(\omega) = \frac{P(\omega)}{I(\omega)}$$

Fig. 8 shows the electro chemical impedance spectrum. The impedance decreases slightly with increasing frequency, as the slope of the current PSD is steeper than -1. The mean value of the electrochemical noise impedance decreased with time and the correlation coefficient also decreased with immersion time. This techni-
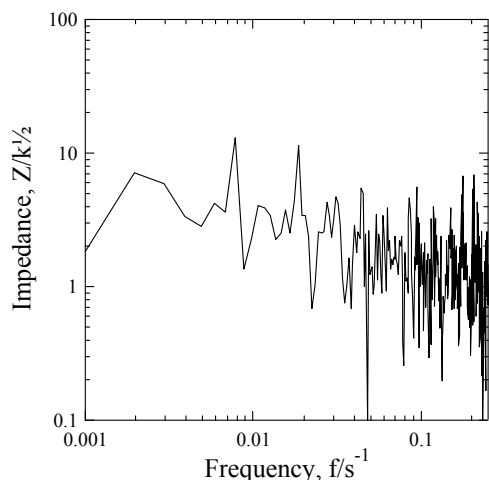
**Fig. 8.** The electro chemical impedance spectrum.

que allow us to measure electrochemical impedance during localized corrosion, which area of dissolution is changed.

## 4. Conclusions

A new type of electrochemical random signal analysis was applied to galvanic corrosion of aluminum alloy specimens with anodic oxide film. The following conclusions can be drawn:

During the incubation period, the initial current and potential values change only slightly with time. When localized corrosion has started, however, these values change suddenly and continuously with fluctuations. The potential and the current fluctuations show a close correlation.

The slope of the potential PSD spectra of the anodized specimens is about minus one (-1) after the localized corrosion has started. The random signal technique employed for makes it possible to measure the electrochemical impedance during localized corrosion and the values do not change with frequency.

## References

1. K. Watanabe, M. Sakairi, H. Takahashi, S. Hirai, and S. Yamaguchi, *J. Electroanal. Chem.*, **473**, 250 (1999).
2. Y. Li, S. Shigyo, M. Sakairi, H. Takahashi, and M. Seo, *J. Electrochm. Soc.*, **144**, 866 (1997).
3. M. Sakairi, P. Skeldon, G. E. Thompson, G. C. Wood, and K. Stevens, *Proc. of ASST 2000*, 410 (2000)
4. M. Sakairi, P. Skeldon, G. E. Thompson, G. C. Wood, andens, *Electrochem. Soc. Proc.*, **99**, 171 (1999).
5. Y. Baba, Oxide film by electrolysis, Maki-Syoten, 28, (1996).
6. Y. Takashima, K. Miwa, M. Sakairi, and H. Takahashi, *J. Surf. Fin. Soc. Jpn.*, **51**, 625 (2000).
7. M. Sakairi, Z. Kato, S. Chu, H. Takahahshi, Y. Abe, and N Katayama, *Electrochemistry*, **71**, 920 (2003).
8. S. Z. Chu, M. Sakairi, and H. Takahashi, K. Shimamura and Y. Abe, *J. Electrochme. Soc.*, **147**, 2181 (2000)
9. T. Kikuchi, M. Sakairi, H. Takahashi, Y. Abe, and N. Katayama, *Surface and coatings technology*, **169**, 199 (2003).
10. T. Kikuchi, M. Sakairi, and H. Takahashi, *J. Electrochem. Soc.*, **150**, C567 (2003).
11. T. Kikuchi, M. Sakairi, H. Takahashi, Y. Abe, and N. Katayama, *J. Electrochem. Soc.*, **148**, C740 (2001).
12. T. Yanagishita, Y. Tomabechi, K. Nishio, and H. Masuda, *Langmuir*, **20**, 554 (2004).
13. F. Matsumoto, K. Nishio, T. Miyasaka, H. Masuda, Jpn. *J. App. Phys. 2-Letters & Express Letter*, **43**(5A), L640 (2004).
14. H. Masuda, F. Matsumoto, and K. Nishio, *Electrochemistry*, **72**, 389 (2004).
15. U. Bertocci, C. Gabrielli, F. Huet, and M. Keddam, *J. Electrochem. Soc.*, **144**, 31 (1997).
16. U. Bertocci, C. Gabrielli, F. Huet, M. Keddam, and P Rousseau, *J. Electrochem. Soc.*, **144**, 37 (1997).
17. T. Tsuru and M. Yaginuma, *Zairyo-to-Kankyo*, **52**, 488 (2003).
18. H. Yashiro, M. Kumagai, and M. Kumagai, *Zairyo-to-Kankyo*, **52**, 466 (2003).
19. Y. Ioti, S. Take, and Y. Okuyama, *Zairyo-to-Kankyo*, **52**, 471 (2003).
20. H. Inoue, M. Kinoshita, and Y. Maeda, *Zairyo-to-Kankyo*, **52**, 483 (2003).
21. Y. Yoneda and H. Inoue, *Zairyo-to-Kankyo*, **52**, 495 (2003).
22. M. Sakairi and Y. Shimoyama, *Electrochemistry, Electrochemistry*, **74**, 458 (2006).
23. M. Sakairi and Y. Shimoyama, submitted to *J. JSEM*.
24. S. -M. Moon, M. Sakairi, and H. Takahashi, *J. Electrochem. Soc.*, **150**, B473 (2003).